Matrix metalloproteinase-9 deficiency phenocopies features of preeclampsia and intrauterine growth restriction

Vicki Plaks[a,1], Julie Rinkenberger[a,1,2], Joanne Dai[a], Margaret Flannery[a], Malin Sund[b,3], Keizo Kanasaki[b,4], Wei Ni[c], Raghu Kalluri[d], and Zena Werb[a,5]

[a]Department of Anatomy, University of California, San Francisco, CA 94143; [b]Division of Matrix Biology, Department of Medicine, Beth Israel Deaconess Medical Center, Harvard Medical School, Boston, MA 02115; [c]Department of Medicine and Diabetes Center, University of California, San Francisco, CA 94143; and [d]Department of Cancer Biology, Metastasis Research Center, University of Texas MD Anderson Cancer Center, Houston, TX 77030.

Contributed by Zena Werb, May 27, 2013 (sent for review April 3, 2012)

The pregnancy complication preeclampsia (PE), which occurs in approximately 3% to 8% of human pregnancies, is characterized by placental pathologies that can lead to significant fetal and maternal morbidity and mortality. Currently, the only known cure is delivery of the placenta. As the etiology of PE remains unknown, it is vital to find models to study this common syndrome. Here we show that matrix metalloproteinase-9 (MMP9) deficiency causes physiological and placental abnormalities in mice, which mimic features of PE. As with the severe cases of this syndrome, which commence early in gestation, MMP9-null mouse embryos exhibit deficiencies in trophoblast differentiation and invasion shortly after implantation, along with intrauterine growth restriction or embryonic death. Reciprocal embryo transfer experiments demonstrated that embryonic MMP9 is a major contributor to normal implantation, but maternal MMP9 also plays a role in embryonic trophoblast development. Pregnant MMP9-null mice bearing null embryos exhibited clinical features of PE as VEGF dysregulation and proteinuria accompanied by preexisting elevated blood pressure and kidney pathology. Thus, our data show that fetal and maternal MMP9 play a role in the development of PE and establish the MMP9-null mice as a much-needed model to study the clinical course of this syndrome.

ectoplacental cone | fetus

Preeclampsia (PE) is one of the most common pregnancy complications worldwide, affecting ~3% to 8% of all pregnancies, and is a leading cause of perinatal and maternal morbidity and mortality (1). PE is characterized by placental hypoperfusion and shallow trophoblast invasion of uterine blood vessels (2) that is particularly evident in the severe cases that commence early in pregnancy (3). Adequate trophoblast invasion is vital to provide the embryo with access to oxygen and nutrients, and, in human and mouse, the placenta is thereby in direct contact with maternal blood. The clinical diagnostic criteria of this syndrome include widespread maternal endothelial dysfunction as evidenced by hypertension, proteinuria, and peripheral and/or cerebral edema (4). In addition to the maternal signs, PE is also frequently associated with intrauterine growth restriction (IUGR) and prematurity (5). The etiology of PE is unclear and the only known cure is delivery of the placenta. The upstream regulatory mechanisms remain elusive, as do the downstream consequences that lead to the maternal signs. Nevertheless, there is substantial evidence for contributing factors including abnormal placentation, particularly the invasive component. Restricted invasion is thought to be a reflection of defects in the cytotrophoblast (CTB) differentiation pathway that is required for uterine interstitial and endovascular invasion. Specifically, CTBs, which are epithelial cells of ectodermal origin, acquire vascular-like properties, and this transformation is dysregulated in PE (3, 6). The rudimentary endovascular invasion is thought to lead to the release of pathologic factors such as vasculogenic and angiogenic substances and their inhibitors into the maternal circulation (2). These factors can induce an inflammatory response as well as generating reactive oxygen and nitrogen species within the vasculature, resulting in the maternal symptoms of PE.

Among the factors that may facilitate trophoblast invasion are matrix metalloproteinases (MMPs) (7). MMPs are well-established mediators of tissue remodeling and angiogenesis, several of which exhibit modified expression in placentas of patients with PE. MMPs target the extracellular matrix (ECM) and are involved in normal physiology and in various pathologies. MMPs are secreted as inactive proenzymes that are activated when cleaved by extracellular proteinases (8). A remarkably broad spectrum of MMPs and tissue inhibitors of MMPs are expressed at the human fetomaternal interface, specifically by uterine natural killer cells, decidual cells, and trophoblasts (9). Their significance in mediating placental development is bolstered in results of in vitro experiments that used a broad-spectrum pharmacological MMP inhibitor (10). MMP9 (92-kDa gelatinase B or type IV collagenase) is a key effector of ECM remodeling that degrades types IV, V, and IX collagens, denatured collagens (gelatin), and elastin (8). Active MMP9 is highly expressed at the embryo implantation site by human and mouse trophoblasts, and is implicated in their invasive behavior (10, 11). Multiple lines of evidence point to a role for MMP9 in PE, as CTBs in PE produce less MMP9 (12) and MMP9 inhibition or gene silencing blocks CTB invasion in vitro (13). MMP9 is also consistently deficient in the plasma of patients with PE (14), and, recently, an MMP9 variant was shown to be a useful biomarker of susceptibility to severe PE and its early onset (15).

Accordingly, we investigated the role of embryonic and maternal MMP9 in embryo implantation and placentation.

Results

MMP9-Null Placentas and Fetuses Exhibit Severe Abnormalities. We first confirmed the previously reported fertility disorders associated with MMP9 insufficiency (16) in several mouse backgrounds. For pure or mixed 129SV/J backgrounds, we observed as much as a 20% reduction in litter size in MMP9-null homozygous matings. For C57BL/6J, we observed as much as a 50% reduction in litter size in homozygous × heterozygous matings, similar to that observed for homozygous matings (16). Heterozygous matings resulted in the expected Mendelian frequency for all genotypes in all backgrounds

Author contributions: V.P., J.R., R.K., and Z.W. designed research; V.P., J.R., J.D., M.F., M.S., K.K., and W.N. performed research; V.P., J.R., J.D., M.F., M.S., K.K., and W.N. analyzed data; and V.P. and Z.W. wrote the paper.

The authors declare no conflict of interest.

[1]V.P. and J.R. contributed equally to this work.

[2]Present addresses: Bayer HealthCare, Berkeley, CA 94701.

[3]Present addresses: Department of Surgery, Umea University, SE-90185 Umea, Sweden.

[4]Present addresses: Department of Diabetology and Endocrinology, Kanazawa Medical University, Uchinada 920-0293, Japan.

[5]To whom correspondence should be addressed. E-mail: zena.werb@ucsf.edu.

This article contains supporting information online at www.pnas.org/lookup/suppl/doi:10.1073/pnas.1309561110/-/DCSupplemental.

tested, similar to that of C57BL/6 and pure 129SV/J (16). In keeping with the previous observations, we conclude that MMP9 should be eliminated from maternal and fetal sides to observe subfertility characterized by reduced litter size.

We examined MMP9-null placentas at embryonic day (E) 10.5, the first time point during pregnancy at which the mature placenta is fully formed with its two distinct layers: labyrinth and junctional zone, which are integrated with the decidua (2). To eliminate the contribution of maternal MMP9, we studied MMP9 null × null matings. We observed runted, pale, and poorly developed MMP9-null embryos (Fig. 1 *A* and *B*). The implantation chambers were reduced in size, and the runted embryos exhibited significantly reduced weight characteristic of IUGR (Fig. 1*C*). We also observed many resorptions in MMP9-null litters but rarely in WT litters.

Placentas from the runted conceptuses were significantly smaller (Fig. 1 *D* and *F*; quantified in Fig. 1*H*). WT placentas had a single layer of trophoblast giant cells (TGCs; Fig. 1 *G* and *E*) that was significantly expanded to multiple layers in MMP9-null placentas (Fig. 1*G*; quantified in Fig. 1*I*). In contrast, the spongiotrophoblasts (STs) and the labyrinthine layer were significantly reduced in the runted placentas (Fig. 1 *E* and *G*; quantified in Fig. 1*I*).

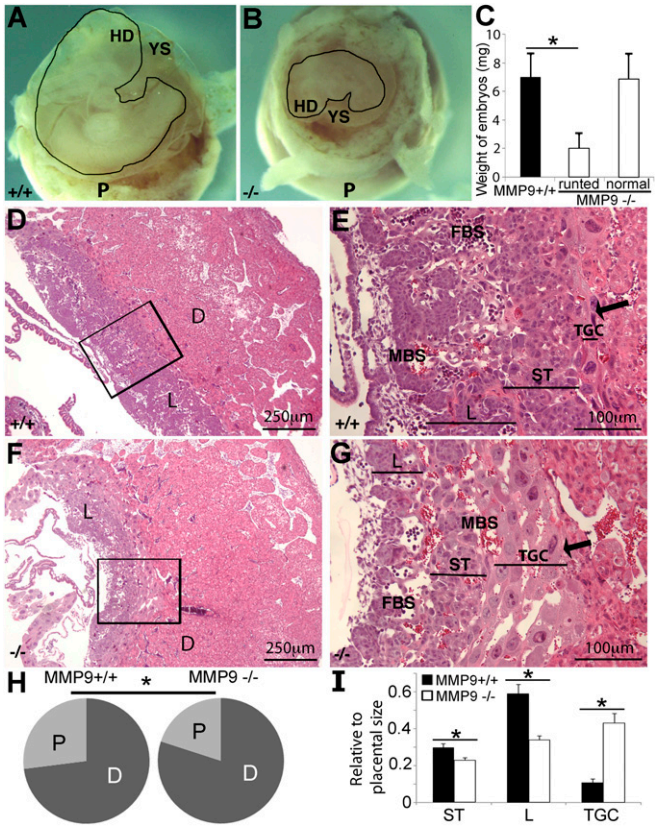

Fig. 1. Placental abnormalities in E10.5 MMP9-null placentas. Animals were mated for 2 h/d to synchronize embryonic development. Representative E10.5 embryos from MMP9 WT × WT ($^{+/+}$) (*A*) and from null × null ($^{-/-}$) (*B*) matings, inside the yolk sac and resting on top of the placenta. The embryos are depicted with a black line. (*C*) A total of 18.4% of the embryos from $^{-/-}$ matings were runted compared with embryos from $^{+/+}$ matings at E10.5 (n = 6 null and n = 4 WT pregnant mice). (*D* and *F*) Placental transverse midsections of WT and runted null E10.5 embryos, respectively. Box demarcates the enlarged area seen in *E* and *G*, respectively. D, decidua; FBS, fetal blood sinus; HD, head; L, labyrinth; MBS, maternal blood sinus; P, placenta; YS, yolk sac. Arrows indicate multiple layers of TGCs in runted $^{-/-}$ vs. single normal layer in $^{+/+}$ placentas. (*H*) Pie charts of placenta (labyrinth, STs, TGCs) vs. decidua lengths calculated from the total length of implantation chambers of each genotype. The $^{-/-}$ placentas were 20% of the entire length of the implantation chamber vs. 27% in $^{+/+}$ (*P = 0.002, n = 6 placentas per genotype). (*I*) Length of labyrinth and ST layers relative to total placental length of each genotype was significantly decreased in $^{-/-}$ placentas; the opposite was for TGC (*P < 0.02).

Before Placental Maturation, MMP9 Null Mice Exhibit Abnormalities in Embryonic Development and Formation of the Maternal–Fetal Interface. MMP9 production by TGCs and its subsequent activation is a prerequisite for trophoblast invasion in vitro. Our group showed previously that MMP9 is produced by the blastocyst and is first detected at the E5.5 implantation site (10). Its expression peaks in TGCs invading the decidua between E7.5 and E8.5 (17) and then decreases to low but detectable levels at E10.5 (18). To determine whether the delayed development evident in MMP9-null placentas at E10.5 stems from an earlier defect, we examined the initial stages of trophoblast invasion. Considering that severe cases of PE are characterized by shallow trophoblast invasion and IUGR, which commences as early as the second trimester in humans (19), we examined E7.5 implantation sites (Fig. 2). MMP9-null implantation sites and the embryos proper were significantly reduced in size. By using timed pregnancies from mice that were mated and plugs checked during a 2-h time window, followed by a morphometric analysis of histological sections of implantation sites, we observed that embryos in all null implantation sites (Fig. 2 *C*, *E*, and *G*) lagged 6 to 12 h behind their WT counterparts (Fig. 2*A*; quantified in Fig. 2*I*).

As the first migratory cell type in the mouse embryo, parietal endoderm (PED) cells synthesize and deposit components of the Reichert membrane, a basement membrane that lies between the PED and the trophectoderm. As the embryo continues to grow (after PED ceases migration at E6.5), new PED cells are derived from the transdifferentiation of borderline visceral extraembryonic endoderm cells. PED is a source for MMP9 secretion, and MMP9 regulates PED differentiation and migration (20). We observed impaired PED migration and expansion along with that of the visceral endoderm in MMP9-null embryos (Fig. 2 *A* and *B* vs. *C*–*H*). Thus, impaired PED and visceral endoderm migration may hamper the migration of trophoblasts from the extraembryonic ectoderm to the base of the EPC and play a role in the developmental delays observed for E7.5 MMP9-null embryos.

TGCs have intense phagocytic activity, leading to the erosion and displacement of the uterine epithelial and decidual cells (21). In the absence of MMP9, the matrix surrounding the decidual cells that is normally engulfed by TGCs failed to be cleared, leading to excessive debris. We detected misoriented ectoplacental cones (EPCs) accompanied by blood pools around the EPC areas that were filled with debris between the tip of the EPC and the mesometrial decidua in MMP9-null embryos (Fig. 2*B* vs. *D*, *F*, and *H*), similar to fibrin accumulation typical of PE placentas (22). Moreover, among various characteristics indicative of the depth of trophoblast invasion, MMP9 nulls exhibited 34% smaller EPC areas than WT (Fig. 2*I*).

MMP9 Deficiency is Associated with Impaired Trophoblast Differentiation and Maternal Vascular Defects. Next, we examined MMP9-null EPCs to determine the cause of these early defects in trophoblast invasion. The EPC commences its growth from the extraembryonic ectoderm at E5.5. The base of the EPC comprises precursor cells that, as they migrate to the tip of the cone, differentiate first into intermediate cells, then into secondary giant cells and later into STs (23). TGCs make initial contacts with the maternal blood sinuses that form in the decidua at E7.5 (21). We did not observe significant differences in proliferation (Fig. 3*A* and Fig. S1*A*) or apoptosis (Fig. 3*B* and Fig. S1*B*) of MMP9-null EPCs compared with age-matched WT EPCs. As the cells migrated from the base of the cone and began to differentiate into invasive trophoblasts, they increased in size. The secondary giant cells that will form connections with the maternal blood sinuses not only enlarge, but cease to proliferate, form focal adhesions, and undergo endoreduplication of their DNA (24). We observed that differentiation of MMP9-null E7.5 EPCs was impaired, as the trophoblast vascular bed length was

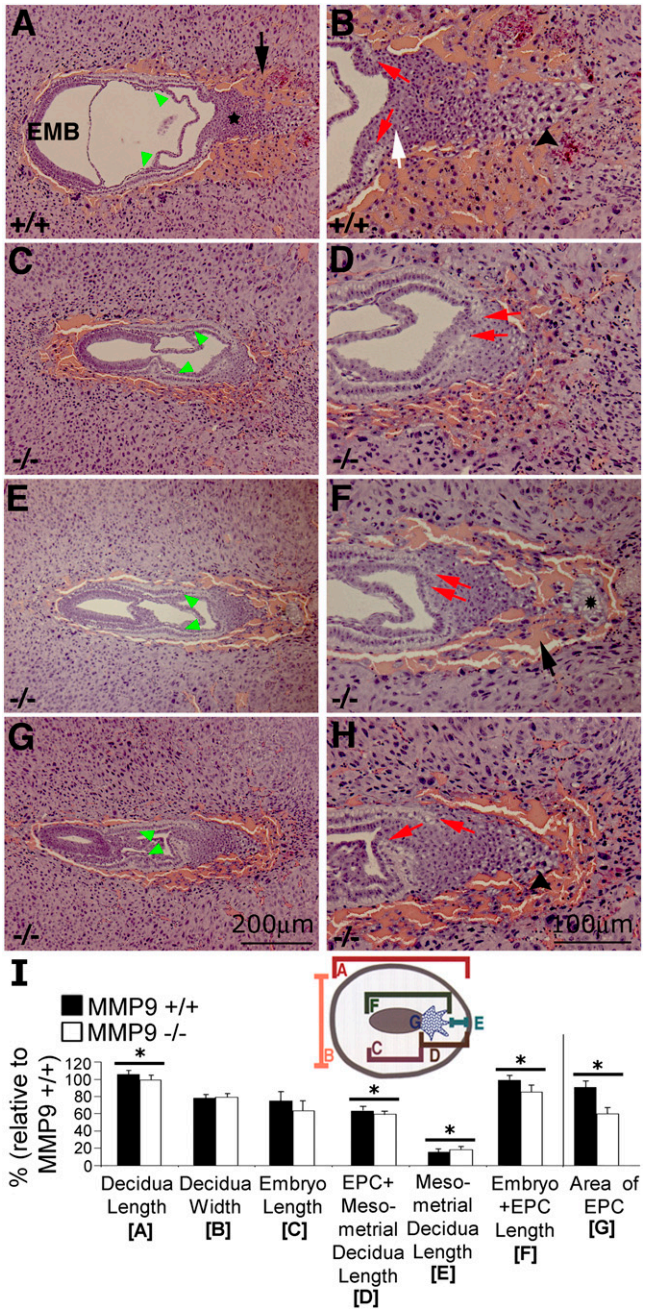

Fig. 2. MMP9-null pregnancies exhibit impaired embryonic development and maternal-to-fetal connections as early as E7.5. Midtransverse sections through E7.5 WT × WT ($^{+/+}$) and null × null ($^{-/-}$) implantation sites were stained with H&E. (*A*) WT embryo with EPC (star), the network of blood channels forming between embryonic trophoblasts and maternal blood sinuses shown (black arrow). (*B*) Enlargement of the EPC area from *A*. The black arrowhead points to mature trophoblasts and the white arrow indicates the trophoblast stem cell layers at the base of the EPC. (*C*, *E*, and *G*) Embryos from MMP9 $^{-/-}$ implantation sites at E7.5. (*D*, *F*, and *H*). Enlargements of EPCs from embryos in *C*, *E*, and *G*, respectively. The embryo in *C* and *D* shows the twisted alignment of the EPC and embryo within the implantation site but near-normal development of the blood channels around the cone. The embryo in *E* and *F* exhibits normal alignment but an EPC area with few mature cells forming blood channels (black arrow). The asterisk indicates a debris plug that may block the formation of trophoblast to maternal blood sinus connections. The embryo in *G* and *H* shows the null phenotype with respect to EPC development. (*H*) Arrowhead shows more mature trophoblasts in the EPC, but a poorly developed network of blood channels. In all null embryos, the visceral endoderm and Reichert membrane plus PED were abnormal (red arrows show tips of visceral endoderm and green arrowheads show tips of Reichert membrane and PED). (*I*) Morphometric analysis of E7.5 embryos, deciduas, and EPCs. Cartoon indicates the parameters measured ($n = 10$ embryos each for $^{-/-}$ and $^{+/+}$; $^{*}P < 0.007$). Percentages are relative to $^{+/+}$ embryo plus EPC (*F*) length for all and relative to $^{+/+}$ area for EPC area (*G*).

significantly reduced in length (Fig. 3*C*). This was corroborated by significantly reduced platelet endothelial cell adhesion molecule-1 (PECAM-1/CD31) immunostaining in MMP9-null embryos (Fig. 3*D*). We also observed that WT E7.5 implantation sites lost E-cadherin expression in EPC cells (Fig. 3*E*). By contrast, MMP9-null embryos represented a more immature phenotype, as E-cadherin–positive cells were significantly present throughout the entire EPC, except the periphery and the base, where only faint expression was observed. Likewise, in normal human (and rat) pregnancy, invasive trophoblasts that remodel the spiral arterioles down-regulate E-cadherin expression (25), which is maintained in severe PE (26).

Differentiation delays of the MMP9-null embryos were subsequently reinforced at E8.5, as we observed defective expression of transcription factors that are markers of chorion and ST differentiation (Fig. S1 *C*–*J*). In addition, we observed accumulation of the MMP9 substrate, collagen IV, in the primary giant and decidual cell layers surrounding the embryo (Fig. S2). Taken together, we conclude that trophoblasts in the MMP9-null EPC are restricted in their developmental potential, which likely contributes to the placental defects and runted embryos observed at E10.5.

Maternal MMP9 Deficiency Contributes to Disordered Early Placentation. Elimination of maternal and embryonic MMP9 from the implantation site had a significant impact on placental development that was observed already at the early stages of EPC formation. To explore the specific role of maternal MMP9 during early embryonic development, we performed reciprocal embryo transfers as indicated in Table S1. Our data indicate that maternal MMP9 could not rescue the low implantation rates of MMP9-null embryos (Fig. 4*A*), as the implantation rates of the null embryos transferred into null or WT females were significantly reduced, and these were accompanied by some reduction in the pregnancy rates.

Histological examination of the implantation sites indicated that null embryos transferred into WT or null females exhibited shallow invasion of the mature trophoblasts from the EPC into the maternal decidua, as indicated by the presence of small EPCs, blood pools, and debris plugs blocking the invasion of the EPC into the mesometrial pole of the decidua (Fig. 4*B*). The debris plugs were probably caused by the inability of the immature cells at the tips of the EPCs to phagocytose the debris. In this respect, maternal MMP9 was insufficient to rescue the phenotypes caused by the lack of embryonic MMP9 expression. Even WT embryos transferred into null females exhibited higher rates of debris accumulation than WT embryos transferred into WT females, which may suggest that a critical amount of MMP9 is needed—mostly embryonic but also maternal. The presence of blood pools further reinforced the role of maternal MMP9, as null or WT embryos transplanted into null females exhibited increased accumulation of blood around the EPC compared with null or WT embryos transplanted into WT females. The overall rate of abnormal embryos, which included twisted, contorted, or constrained embryos, was also reduced for null embryos transferred into WT females vs. those transferred into null females. Fully resorbed embryos were only detected when null embryos were transferred into null females. Taken together, this analysis indicates that normal embryonic trophoblast development requires MMP9 expression by embryo and mother. However, WT embryos were likely to survive and develop with fewer problems in a null background than in the reciprocal setup, as exemplified by histologic findings (Fig. 4*C*).

MMP9-Null Mothers Carrying Null Fetuses Exhibit Clinical Diagnostic Features of PE. Our study shows that both maternal and embryonic MMP9 play roles in contributing to adequate trophoblast invasion

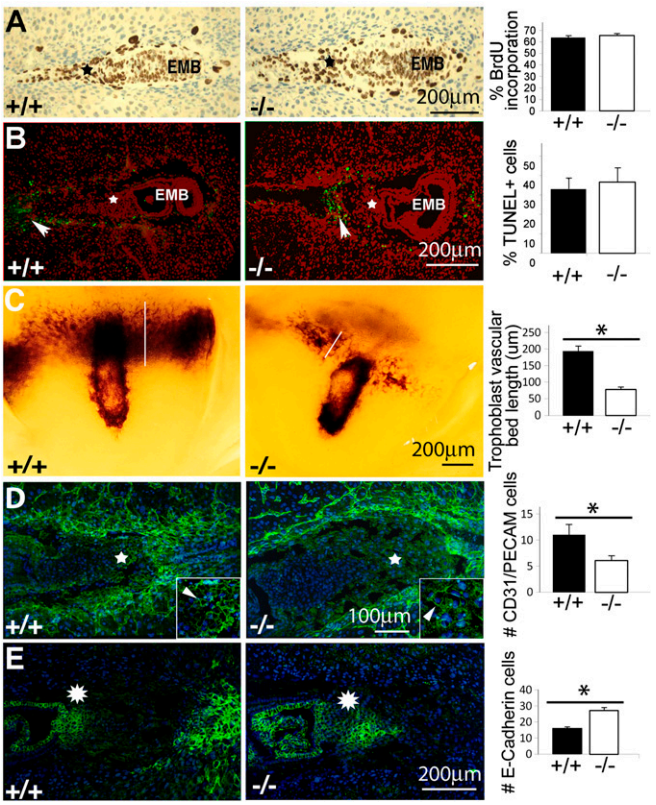

Fig. 3. MMP9-null conceptuses exhibit changes in the vascular bed length and delayed differentiation but no significant perturbations in trophoblast proliferation and apoptosis. (*A*) BrdU staining (brown) postincorporation into WT × WT ($^{+/+}$) and null × null ($^{-/-}$) implantation sites determined at E6.5. EPCs are marked by stars. EMB, embryo. (*B*) TUNEL staining (green) of E7.5 $^{+/+}$ and $^{-/-}$ implantation sites. Nuclei are stained with propidium iodide (red). EPCs marked by stars (n = 10 EPCs for each genotype). (*C*) The trophoblast vascular bed (length of vascular invasion) of null embryos was quantified from the whole mounts, with blood as a measure for functional vessels. The white line depicts the parameter measured. (*D* and *E*) Immunostainings of E7.5 implantation sites are visualized with FITC (green) and nuclei are counterstained with DAPI [blue; n = 5 for each genotype ($^{-/-}$, $^{+/+}$)]. (*D*) CD31/PECAM-1 immunostaining. Star indicates area enlarged (*Insets*) to show difference in cell morphology (*P < 0.005). (*E*) E-cadherin immunostaining. Asterisk indicates the area of the cone nearest the embryo where E-cadherin–positive cells are located (*P < 0.005).

and placentation. We next focused on the effect that MMP9 deficiency has on the pregnant mother. Taking into account that the maternal effect was more pronounced in C57BL/6J (*Materials and Methods*), we chose a mating scheme that aimed for the mothers to carry equal frequencies (50%) of heterozygous versus null (i.e., MMP9-deficient) or WT (i.e., MMP9-sufficient) fetuses. The heterozygous fetuses were especially important in the MMP9-deficient group, to potentially maintain pregnancy so that we could examine parameters relevant to a pregnancy state even if the null mothers carried defective MMP9-deficient conceptuses.

We first confirmed the placental and fetal phenotype in this background. At the end of pregnancy (E20.5), ∼30% of MMP9-null fetuses were found dead. Relating these data to fetal demise in PE, the fetuses had not been dead for more than 24 h. Macroscopically, these fetuses appeared pale and smaller than their healthy littermates. Resembling characteristics of PE, placentas of dead MMP9-null fetuses had significantly reduced numbers of TGCs at the border region between the labyrinth and the STs (Fig. 5*A*; quantified in Fig. 5*C*) as well as at the border region between the STs and the decidua (Fig. 5*B*; quantified in Fig. 5*D*). We also confirmed the early manifestation of placental MMP9-null impaired phenotype in this background at E8.5 (Fig. S3*A*). We then correlated the placental phenotype with changes in maternal serum VEGF and urine protein levels. VEGF is critically involved in placental vascular patterning and invasion of CTBs. The perturbed VEGF levels found in PE are attributed to the dysfunctioning placenta (27). At present, the most promising biomarkers for PE are the soluble forms of the type-1 VEGF receptor (sFlt1) and endoglin, which increase dramatically in the blood of affected women weeks before the onset of clinical symptoms (28). A relative concomitant decrease in VEGF and placental growth factor has also been reported (29). In mice, low levels of circulating VEGF induce proteinuria (i.e., increased urine protein levels), both of which are indicative of PE in women (30). We observed that pregnant MMP9-null dams had lower serum levels of total VEGF at E12.5 of pregnancy that returned to normal levels by postpartum day (P) 10 (Fig. 5*E*). As previously observed for down-regulated circulating VEGF (30), MMP9-null mice exhibited gestational proteinuria by E13.5 that peaked at E18.5 and returned to baseline levels by P10 (Fig. 5*F*). Moreover, elevated blood pressure (BP) in MMP9-null females was exhibited throughout the pregnancy, but also before implantation, and correlated with lack of born pups (Fig. 5*G*). Significantly increased systolic BP was also exhibited in the preimplantation phase of MMP9-null females that had pups, but did not persist, supporting the fact that elevated BP is associated with fetal loss in this cohort. Furthermore, MMP9-null females exhibited significantly elevated systolic BP before pregnancy (123.4 ± 0.02 mm Hg) vs. MMP9$^{+/-}$ (115.5 ± 0.72 mm Hg; P = 0.003). Indicative of kidney pathology similar to glomerular endotheliosis, the null females exhibited reduced percentage of glomeruli with open capillaries (Fig. 5*H*), without significant impairment of their size or density (Fig. S3 *B* and *C*). We conclude that numerous pathologies exhibited in PE and IUGR are phenocopied in MMP9-null pregnant mice (Table S2).

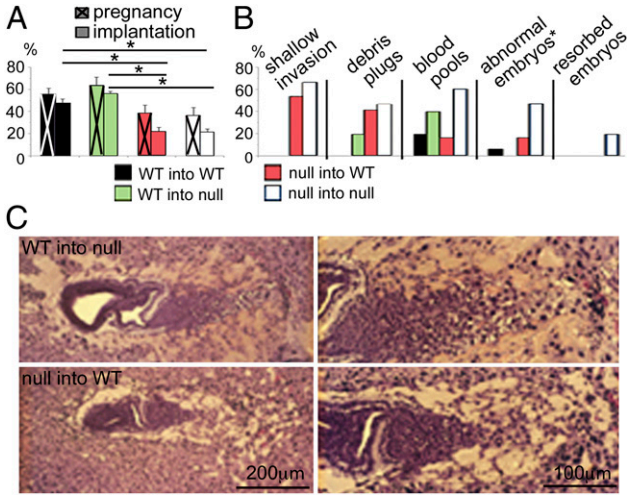

Fig. 4. Maternal MMP9 contributes to the establishment of the maternal-to-fetal connections. (*A*) Pregnancy rates (*Left*, X-marked columns; percentage of pregnant females among total females transferred with embryos) and implantation rates (*Right*; percentage of implantation sites detected among total embryos transferred) of null embryos transferred into WT or null females exhibit lower values than WT embryos (*P < 0.0001). (*B*) Implantation sites from embryos transfers between WT and null females exhibit multiple abnormalities including shallow trophoblast invasion resulting in blood pools around the EPCs and embryos, debris plugs resulting in abnormal embryos, and resorptions. (*Twisted, contorted, and constrained.) (*C*) Histological sections exemplify the defects of WT and null embryo transfers into females of the reciprocal genotype, with a severe phenotype in null embryos, exhibiting shallow invasion of immature-appearing trophoblasts. Number of EPCs and embryos analyzed by histology: WT into WT, n = 15/45; WT into null, n = 5/63; null into WT, n = 24/33; null into null, n = 15/33.

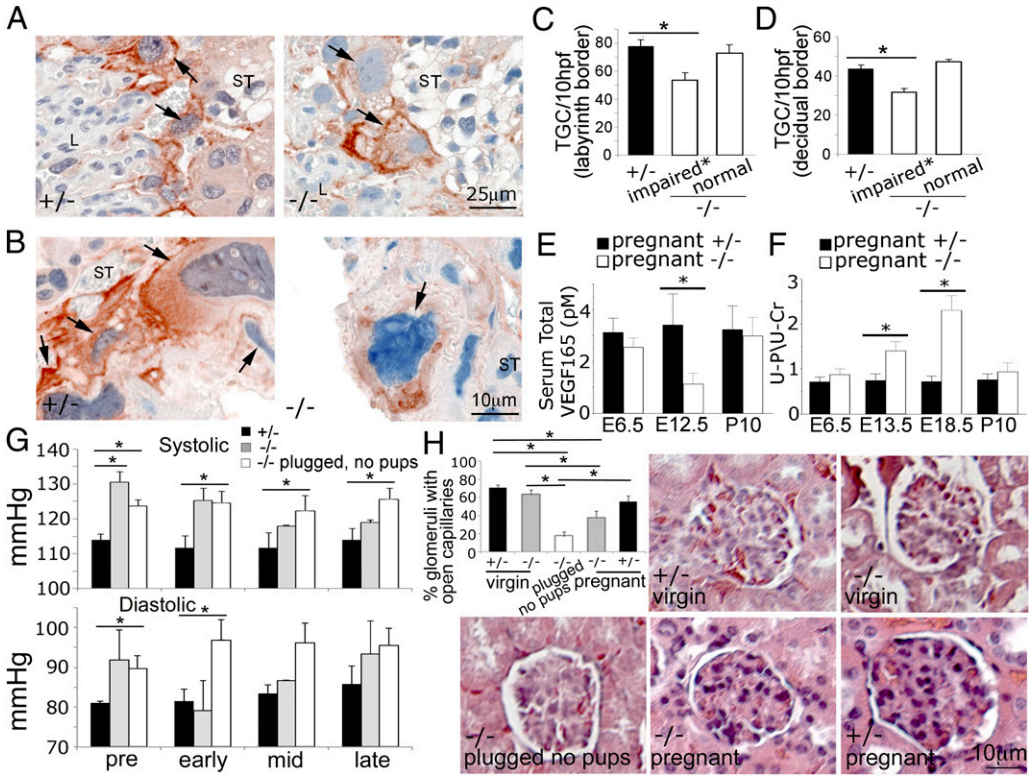

Fig. 5. Pregnant MMP9-null mice exhibit clinical diagnostic features of PE. Cytokeratin staining of TGCs (arrows) from E20.5 placentas in control ($^{+/-}$) and MMP9-null ($^{-/-}$) mice on (*A*) the inner border of the ST layer (labyrinth border) or (*B*) the outer border of the ST layer (decidual border). Number of TGCs found in the placentas of the impaired $^{-/-}$ fetuses at (*C*) the labyrinth border or (*D*) the decidual border was significantly reduced (*$P = 0.04$ and $P = 0.02$, respectively). L, placental labyrinth. [*Aborted, dead after Caesarean (C) section.] (*E*) Total VEGF165 levels in sera collected from pregnant mice were significantly reduced in $^{-/-}$ at E12.5 and returned to control levels at P10. (*F*) Urine protein/creatinine level ratio (U-P/U-Cr) was significantly elevated in $^{-/-}$ at E13.5 and E18.5 but back to control levels by P10. (*G*) BP measurements reveal that $^{-/-}$ mice exhibit elevated BP during the pregnancy time period associated with lack of pups (C-sectioned on E18.5); pre-, before implantation until E4.5; early-, E4.5 to E7.5; mid-, E12.5 to E15.5; late-, E17.5 to E18.5. MMP9$^{+/-}$ and MMP9$^{-/-}$ are pregnant females that had pups on E18.5 [$n = 7$ MMP9$^{+/-}$ (7.2 pups plus 0.3 resorptions per female), $n = 2$ MMP9$^{-/-}$ (five pups plus one resorption per female), and $n = 9$ MMP9$^{-/-}$ plugged, no pups]. (*H*) Percentage of open glomerular capillaries in kidneys of females in *G* was significantly reduced, especially in the $^{-/-}$ plugged, no pups mice but also in $^{-/-}$ that had pups (*$P < 0.0001$). Representative H&E glomeruli images are included (lower-magnification images in Fig. S3C).

Discussion

Our data answer a longstanding question regarding the role of MMP9 in trophoblast invasion and placental development. Moreover, we phenotypically connect MMP9 insufficiency to early manifestation of PE, characteristic of the more severe cases of this syndrome. Placental defects associated with MMP9 deficiency in mice were evident early, during EPC formation, and attributable to defective trophoblast differentiation. Similar to MMP9-null mice that exhibit impaired embryo development, early-onset forms of PE in women are almost always associated with IUGR and early manifestation of reduced placental volume. Moreover, MMP-null pregnant mice exhibit diagnostic criteria for PE as VEGF dysregulation and proteinuria, on the background of preexisting elevated BP and signs of kidney pathology.

At E7.5, before the placenta had formed, all MMP9-null embryos exhibited delayed development linked to impaired endometrial decidualization and trophoblast invasion, resulting in poorly developed maternal–fetal vascular connections. The observed morphological and molecular alterations, which included delayed PED and Reichert membrane migration and expansion, likely contributed to the developmental delays of the MMP9 embryos and mirror defects in CTB invasion observed in PE (3).

These early effects of the absence of MMP9 probably contributed to the IUGR features of these runted and resorbing embryos detected at E10.5. Although all cell layers were present in the placentas of runted MMP9-null embryos, the TGC layer was significantly enlarged at the expense of the labyrinth and the ST layers. Because, at E10.5, MMP9 is mostly expressed in TGCs (18), its absence may correspond with this abnormal phenotype, although it can also be a compensatory effect for the loss of the labyrinth. The poorly developed labyrinth probably contributed to the runting of MMP9-null embryos by restricting nutrient and gas exchange.

Reciprocal embryo transfers indicated that, although embryonic MMP9 is more dominant, normal embryonic trophoblast invasion and differentiation also require maternal MMP9. These experiments were instrumental in differentiating the role of embryonic from maternal MMP9 because, in most heterozygous matings, in which maternal blood in the decidua contains MMP9, null pups are rescued as they appear in their expected Mendelian frequency. However, given the secreted, non–cell-autonomous nature of MMP9, it is also possible that MMP9 provided by the heterozygous and WT embryos in these heterozygous matings add to threshold levels of MMP9 that, in turn, enabled sufficient vascular development to help sustain the null embryos, resulting in this Mendelian frequency. The suggested threshold MMP9 levels needed to sustain normal litter size were further reinforced in C57BL/6J homozygous × heterozygous matings, which yielded 50% reduction in the size of litters, not all of which were the null fetuses (as analyzed at E20.5).

Our data also demonstrate that, during later stages of pregnancy, the lack of maternal and fetal MMP9 led to decreased serum VEGF, possibly as a result of diminished ECM degradation and failure to release stored VEGF (31). This phenomenon could also contribute to deficient trophoblast endovascular invasion. There is circumstantial evidence that antagonism of VEGF and placental growth factor may have a pathogenic role in the appearance of hypertension and proteinuria. The deficiency in total VEGF may therefore be reflected in an increase in sFlt1, thus leading to the observed proteinuria and hypertension (32). In fact, angiogenic factors are now used to predict PE (1). In addition to sFlt1 as a predictive marker for PE, other markers, which rely on VEGF levels, are being discovered, such as VEGF165b, an antiangiogenic splice variant of VEGF165 that may blunt some of the endothelial effects of VEGF165 (28). This could also explain why the concentration of free, biologically active VEGF

decreases in PE, but total VEGF in PE is still in a large access compared with sFlt1.

We also suggest that MMP9-null mice are a model of PE with preexisting hypertension and kidney pathology. Often, women with a history of hypertension are more susceptible to developing PE upon pregnancy. There is evidence showing that preexisting hypertension can lead to complications of pregnancy such as placental abruption (33), IUGR, and perinatal death (34). Moreover, some MMP9-null mice exhibit kidney pathology and are also more prone to nephritis (35), possibly rendering their kidneys as more sensitive to a challenge like pregnancy.

In summary, as we show here, the cumulative decreases in MMP9 involving mostly the fetal but also the maternal contributions phenocopy aspects of PE accompanied by IUGR in the mouse, and suggest that a threshold level of MMP9 at the maternal–fetal interface is required for normal placentation. So far, no therapy exists that may cure defective trophoblast invasion in women with PE. The discovery of MMP9 as a regulator of this process may offer therapeutic insights to this condition. Even though the mouse and the human maternal–fetal interfaces are morphologically different, they are physiologically similar, hereby suggesting the MMP9-null mice as a model for delineating the yet unknown aspects of PE pathophysiology.

Materials and Methods

Mice Mating Schemes. All animal experiments were approved by the University of California, San Francisco, Institutional Animal Care and Use Committee.

Timed pregnancies. Plug day was set as E0.5. Homozygous matings were used to study the effect of MMP9 total elimination during early placentation using 129SV/J pure or mixed backgrounds, which putatively have a milder phenotype. The effect of MMP9 on the mother, which was more profound in the C57BL/6J background, was examined in MMP9-null females mated with heterozygous males compared with heterozygous females mated with WT males. Additional details are provided in *SI Materials and Methods*.

Reciprocal embryo transfers. Blastocysts were harvested from pregnant MMP9-null or WT females and reciprocally transferred into day-2.5 pseudopregnant hosts, after which the implantation sites were analyzed, as described in *SI Materials and Methods*.

Proliferation and Apoptosis Assays. BrdU incorporation and TUNEL staining were performed by using kits from Zymed laboratories and Trevigen, respectively, as indicated in *SI Materials and Methods*.

Immunohistochemistry and Morphometric Analysis. Stainings were performed by using antibodies and kits from Zymed Laboratories, Pharmingen, Invitrogen, Molecular Probes, and DAKO, and quantified as indicated in *SI Materials and Methods*.

Serum VEGF and Urinary Protein Measurements. The total serum VEGF levels (Quantikine ELISA Mouse VEGF Immunoassay; MMV00; R&D Systems) and urine protein levels (colorimetric assay; Sigma) were measured as previously described (30).

Tail Cuff BP Measurement and Analysis. Mouse BP was measured by using a conventional tail-cuff method as indicated in *SI Materials and Methods*.

Statistics. Significance was determined at $P < 0.05$ by unpaired Student t test for datasets with two groups and by one-way ANOVA followed by Tukey multiple comparison test for datasets with three or more groups.

ACKNOWLEDGMENTS. We thank Dr. Susan Fisher for critical reading; Ying Yu for genotyping; Dr. Zoltan Laszik for kidney histology advice; and Jelena R. Linnemann, Eline C. Van Kappel, Jennifer Tai, and Charlotte D. Koopman for technical help. This work was supported by National Institutes of Health Grants CA057621 (to Z.W.), HD026732 (to Z.W.), CA075072 (to Z.W.), DK55001 (to R.K.), DK081976 (to R.K.), CA125550 (to R.K.), CA155370 (to R.K.), and CA151925 (to R.K.); American Cancer Society Fellowships (to J.R.); Machiah Foundation and Bikura/Israeli Science Foundation postdoctoral fellowships (to V.P.); a Weizmann Institute of Science–National Postdoctoral Award Program for Advancing Women in Science (to V.P.); and a foreign study grant from the Kanae Foundation for the Promotion of Medical Science in Japan (to K.K.).

1. Cerdeira AS, Karumanchi SA (2012) Angiogenic factors in preeclampsia and related disorders. *Cold Spring Harb Perspect Med* 2(11).
2. McMaster MT, Zhou Y, Fisher SJ (2004) Abnormal placentation and the syndrome of preeclampsia. *Semin Nephrol* 24(6):540–547.
3. Naicker T, Khedun SM, Moodley J, Pijnenborg R (2003) Quantitative analysis of trophoblast invasion in preeclampsia. *Acta Obstet Gynecol Scand* 82(8):722–729.
4. Winn VD, Gormley M, Fisher SJ (2011) The impact of preeclampsia on gene expression at the maternal-fetal interface. *Pregnancy Hypertens* 1(1):100–108.
5. Sibai B, Dekker G, Kupferminc M (2005) Pre-eclampsia. *Lancet* 365(9461):785–799.
6. Pijnenborg R, Vercruysse L, Hanssens M (2006) The uterine spiral arteries in human pregnancy: Facts and controversies. *Placenta* 27(9-10):939–958.
7. Lalu MM, Xu H, Davidge ST (2007) Matrix metalloproteinases: Control of vascular function and their potential role in preeclampsia. *Front Biosci* 12:2484–2493.
8. Kessenbrock K, Plaks V, Werb Z (2010) Matrix metalloproteinases: Regulators of the tumor microenvironment. *Cell* 141(1):52–67.
9. Anacker J, et al. (2011) Human decidua and invasive trophoblasts are rich sources of nearly all human matrix metalloproteinases. *Mol Hum Reprod* 17(10):637–652.
10. Alexander CM, et al. (1996) Expression and function of matrix metalloproteinases and their inhibitors at the maternal-embryonic boundary during mouse embryo implantation. *Development* 122(6):1723–1736.
11. Cohen M, Meisser A, Bischof P (2006) Metalloproteinases and human placental invasiveness. *Placenta* 27(8):783–793.
12. Graham CH, McCrae KR (1996) Altered expression of gelatinase and surface-associated plasminogen activator activity by trophoblast cells isolated from placentas of preeclamptic patients. *Am J Obstet Gynecol* 175(3 pt 1):555–562.
13. Librach CL, et al. (1991) 92-kD type IV collagenase mediates invasion of human cytotrophoblasts. *J Cell Biol* 113(2):437–449.
14. Kolben M, et al. (1996) Proteases and their inhibitors are indicative in gestational disease. *Eur J Obstet Gynecol Reprod Biol* 68(1-2):59–65.
15. Rahimi Z, Rahimi Z, Shahsavandi MO, Bidoki K, Rezaei M (2013) MMP-9 (-1562 C:T) polymorphism as a biomarker of susceptibility to severe pre-eclampsia. *Biomarkers Med* 7(1):93–98.
16. Dubois B, Arnold B, Opdenakker G (2000) Gelatinase B deficiency impairs reproduction. *J Clin Invest* 106(5):627–628.
17. Reponen P, et al. (1995) 92-kDa type IV collagenase and TIMP-3, but not 72-kDa type IV collagenase or TIMP-1 or TIMP-2, are highly expressed during mouse embryo implantation. *Dev Dyn* 202(4):388–396.
18. Teesalu T, Masson R, Basset P, Blasi F, Talarico D (1999) Expression of matrix metalloproteinases during murine chorioallantoic placenta maturation. *Dev Dyn* 214(3):248–258.
19. Hafner E, et al. (2003) Placental growth from the first to the second trimester of pregnancy in SGA-foetuses and pre-eclamptic pregnancies compared to normal foetuses. *Placenta* 24(4):336–342.
20. Behrendtsen O, Werb Z (1997) Metalloproteinases regulate parietal endoderm differentiating and migrating in cultured mouse embryos. *Dev Dyn* 208(2):255–265.
21. Bevilacqua EM, Abrahamsohn PA (1988) Ultrastructure of trophoblast giant cell transformation during the invasive stage of implantation of the mouse embryo. *J Morphol* 198(3):341–351.
22. Kanfer A, et al. (1996) Increased placental antifibrinolytic potential and fibrin deposits in pregnancy-induced hypertension and preeclampsia. *Lab Invest* 74(1):253–258.
23. Rossant J, Cross JC (2001) Placental development: Lessons from mouse mutants. *Nat Rev Genet* 2(7):538–548.
24. Parast MM, Aeder S, Sutherland AE (2001) Trophoblast giant-cell differentiation involves changes in cytoskeleton and cell motility. *Dev Biol* 230(1):43–60.
25. Reuss B, et al. (1996) Connexins and E-cadherin are differentially expressed during trophoblast invasion and placenta differentiation in the rat. *Dev Dyn* 205(2):172–182.
26. Zhou Y, et al. (1997) Human cytotrophoblasts adopt a vascular phenotype as they differentiate. A strategy for successful endovascular invasion? *J Clin Invest* 99(9):2139–2151.
27. Zhou Y, et al. (2002) Vascular endothelial growth factor ligands and receptors that regulate human cytotrophoblast survival are dysregulated in severe preeclampsia and hemolysis, elevated liver enzymes, and low platelets syndrome. *Am J Pathol* 160(4):1405–1423.
28. Hertig A, Liere P (2010) New markers in preeclampsia. *Clin Chim Acta* 411(21-22):1591–1595.
29. Fisher SJ (2004) The placental problem: linking abnormal cytotrophoblast differentiation to the maternal symptoms of preeclampsia. *Reprod Biol Endocrinol* 2:53.
30. Sugimoto H, et al. (2003) Neutralization of circulating vascular endothelial growth factor (VEGF) by anti-VEGF antibodies and soluble VEGF receptor 1 (sFlt-1) induces proteinuria. *J Biol Chem* 278(15):12605–12608.
31. Bergers G, et al. (2000) Matrix metalloproteinase-9 triggers the angiogenic switch during carcinogenesis. *Nat Cell Biol* 2(10):737–744.
32. Maynard SE, et al. (2003) Excess placental soluble fms-like tyrosine kinase 1 (sFlt1) may contribute to endothelial dysfunction, hypertension, and proteinuria in preeclampsia. *J Clin Invest* 111(5):649–658.
33. Bateman BT, et al. (2012) Hypertension in women of reproductive age in the United States: NHANES 1999-2008. *PLoS ONE* 7(4):e36171.
34. Sibai BM, et al.; National Institute of Child Health and Human Development Network of Maternal-Fetal Medicine Units (1998) Risk factors for preeclampsia, abruptio placentae, and adverse neonatal outcomes among women with chronic hypertension. *N Engl J Med* 339(10):667–671.
35. Lelongt B, et al. (2001) Matrix metalloproteinase 9 protects mice from anti-glomerular basement membrane nephritis through its fibrinolytic activity. *J Exp Med* 193(7):793–802.